Functionalization of self-organized networked $SiO_xH_yC_z$ nano-islands deposited by atmospheric pressure microwave plasma torch on Pt/Si(100) substrates patterned by nano-indentation

Xavier Landreau[1], Benjamin Boëns[2], Briac Lanfant[1], Thérèse Merle[1], Guillaume Bouscarrat[3], Christelle Dublanche-Tixier[1], Rachida Zerrouki[2], Pascal Tristant[1]

[1]SPCTS, 12 Rue Atlantis, Ester Technopole, 87068 Limoges, France
[2]LCSN, 123 Avenue Albert Thomas, 87060 Limoges Cedex, France
[3]CITRA, ENSIL, 16 Rue Atlantis, Ester Technopole, 87068 Limoges, France

ABSTRACT

A coaxial injection microwave excited plasma torch operating at atmospheric pressure is applied to synthesizing $SiO_xH_yC_z$ nano-islands from hexamethyldisiloxane precursor on prepatterned Pt/Si(100) substrates. Herein we report on the spatial organization of these nano-islands in a square array of indents. Prior to the PECVD deposition, the Pt/Si(100) substrates are patterned by nano-indentation. SEM characterizations demonstrate that nano-indents act as trapping sites, allowing ripening of $SiO_xH_yC_z$ nano-dots at those locations during subsequent deposition and diffusion of chemical species on the surface. Results show that islands ordering is intrinsically linked to the nucleation and growth at indented sites and strongly depends on pattern parameters. Then, we report on the selective alkyno-functionalization of the nano-islands surface, followed by the addition of coumarin fluorophore through click-chemistry process for a sensing purpose.

Keywords: PECVD, $SiO_xH_yC_z$ nano-islands, nano-indentation, self-organization, functionalization

1 INTRODUCTION

In a previous work, we demonstrated the preferential growth and ordering ability of $SiO_xH_yC_z$ islands in a square array of indents patterned by nanoindentation on Si (100) substrates [1, 2] maintained at a 30°C surface temperature. Referring to the deviation of the spatial distribution of the $SiO_xH_yC_z$ islands from pure randomless, we concluded that indents act as preferred nucleation sites and that the mobility of these islands on the slope of the pits or at the pit edges is affected by the local minimum energy to such degree as to favor the bonding in the edges. However, despite the preferential growth of large hemispherical islands (~150 nm) in the bottom of the indents, some matter also remains trapped in and between the indents: in particular, smaller dots gather at the edges and on the sidewall slope of the pits.

In direct continuation of this work, $SiO_xH_yC_z$ nano-hillocks are grown from an argon-hexamethyldisiloxane mixture on prepatterned Pt/Si (100) substrates by plasma enhanced chemical vapour deposition process using an axial injection torch (TIA) at atmospheric pressure. The noble metal layer allows to minimize the chemical interactions between the substrate surface and the chemical compounds deposited from the gas phase in such a way to maximize the adatoms surface diffusion length λ_D and optimize the indent filling. Indeed, since spatial island equilibration is triggered by surface diffusion mechanisms, optimal ordering and filling occurs when the pattern pitch is comparable to λ_D.

In a second step, a thorough Fourier Transformed Infra-Red (FTIR) spectroscopy study is performed on $SiO_xH_yC_z$ nano-hillocks with the aim to directly correlate the Si-O-Si vibrators conformation with the morphological and chemical islands properties (compactness, dimensions, native surface functionalization). Besides, indirect information about surface growth mechanisms are obtained. Results demonstrate that the TO_3 vibrational mode (revealing acute Si-O-Si angles) is predominant, reflecting the sharp and pointed nature of the domed-like surface. Concomitantly, strong correlations are established between the islands compactness and the TO_2 mode variations (obtuse Si-O-Si angles) as well the downward diffusion amplitude of the deposited chemical species.

In a last step, we report on the selective alkyno-functionalization of the nano-islands surface, followed by the addition of coumarin fluorophore through click-chemistry process for a sensing purpose.

2 EXPERIMENTAL SECTION

The experimental apparatus, described in detail elsewhere [3,4], consists of a microwave plasma TIA operated by a 2.45 GHz microwave generating magnetron. The microwaves are delivered to the flowing gas in a metallic coaxial tube, through a rectangular waveguide. The absorption of microwave energy in the flowing gas results in formation and sustention of plasma at the exit nozzle. The torch is placed in a large cylindrical deposition

chamber. The substrate is fixed perpendicular to the plasma flow at a constant value of 30 mm. The reactor is equipped with an exhaust at the top to ensure the removal of products. A schematic description of the PECVD system is shown in the Fig. 1.

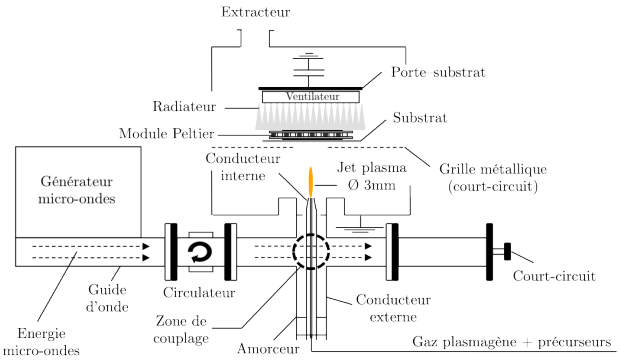

Figure 1: experimental PEVD deposition set-up with the injection axial torch (TIA)

In the present work, silicon oxide nanostructures are deposited keeping the substrate stationary in front of the plasma. The process gases and the precursor display an adequate purity (argon: Nital, 5.0 purity, HMDSO: liquid at standard conditions, Alfa Aesar, 98%). Nanoindentation of Pt/Si(100) substrates has been performed at room temperature using a NanoIndenter XP^{TM} system (MTS Nano Instruments) fitted with a Berkovich diamond tip. A maximum indentation load of 75 mN was used to form residual impressions ~250 nm deep and of ~1500 nm diameter in such a way to cross the top noble metal and disclose the silicon substrate. Three dimensionally ordered square arrays of indents were patterned with pitches ranging from 1 to 3 µm (Fig. 2). Prior to deposition, the pre-patterned substrates were cleaned in a fluorydric acid solution in order to remove the native SiO_x nanometric layer. This protocol allows to obtain an atomically flat surface and also a good surface roughness reproducibility both within and between the different indents.

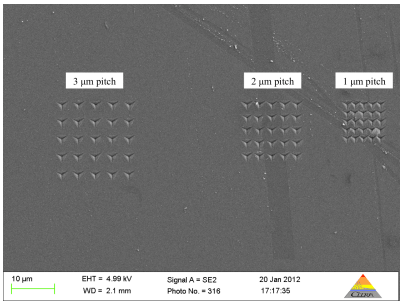

Figure 2: SEM images of the 1, 2 and 3 µm-pitch patterned substrates. Indented arrays prior to $SiO_xH_yC_z$ deposition.

Specular Reflexion Fourier Transform Infra-Red (SR-FTIR) spectroscopy analyses (Nicolet 6700, resolution of 0.5 cm^{-1}) are performed at the centre area of the deposits. Spectra deconvolutions into Gaussian profiles are realised using the software Peakoc and Origin Pro 7.5. All the reported intensities and wavenumbers are average values on at least 6 repetition samples. Spectra deconvolutions into Gaussian profiles are realized using the softwares OMNIC and Origin Pro 7.5. Intensities of each band are normalized from the TO_1 mode intensity in order to avoid the contribution of the film thickness and to estimate the proportion of different chemical species contained within the film. Then, the surface morphology was investigated by Scanning Electron Microscopy (SEM; Philips XL30).

3 RESULTS AND DISCUSSION

1.1 Ordering of $SiO_xH_yC_z$ nano-islands

In this part, we describe the effective pathway towards an ordered configuration of $SiO_xH_yC_z$ nano-dots on nanoindentation patterned Pt/Si(100) substrates. By the analysis of the evolution of the island assembly, we gain experimental insight into the initial stages of the ordering process induced by nanomechanical patterning. Fig. 3 shows the surface morphology after the initial stages of $SiO_xH_yC_z$ deposition and hillock assembly.

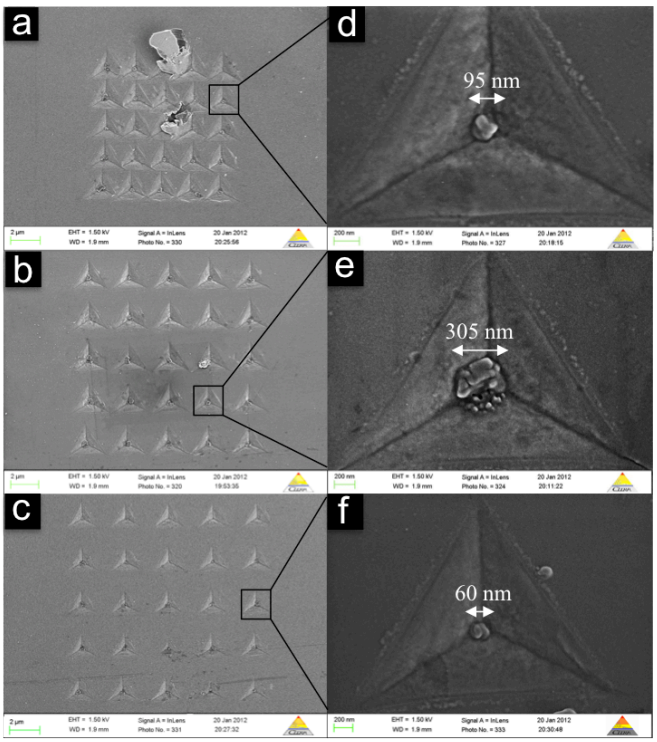

Figure 3: SEM images of $SiO_xH_yC_z$ hemispherical nano-islands localized at the center of nano-indents after 10 s of deposition for a 30°C surface temperature. The top layer between the indents is platinum.

For all patterns, $SiO_xH_yC_z$ nano-dots nucleate inside all indents. Outside the pit region the density of deposited matter first decreases and then flattens far away from the

indent due to a lower stress relaxation and limited chemical interactions with the noble surface [2]. For the 3 µm-pitch array (Fig. 3c and 3f), some matter also remains trapped in and between the indents: in particular, smaller dots gather at the edges and on the sidewall slope of the pits. These two observations reasonably agree with theoretical predictions of [5] suggesting that inside the indents the island formation energy is smaller than on the flat surface, due to an enhanced strain relaxation: because of a higher coordination number, adatoms located at the bottom of an indent (or an edge in a simple case) find a more stable position than those located on a smooth and flat surface. Indeed, each atom reaching at least one edge of an indent can relax to the extent that it finds at least two nearest neighbours within the atoms belonging to the substrate or to an existing island. However, in addition to a pure geometrical effect of the indent, a second effect due to an island already present can greatly modify the diffusion within the indent. Such phenomena is the process by which larger particles grow at the expense of smaller one. After the initial nucleation stage, the molecular clusters exceeding a critical size continue to grow and attract molecules moving on the surface. Then, the islands may progressively grow through large island–small island interactions: the most stable islands can develop a capture zone where the wandering molecules are strongly attracted. In our case, the stable islands located at the center of the indents represent the most favourable energetic sites for new impinging molecules or for small adparticles already present.

For the 1 µm-pitch array (Fig 3a), despite a good filling of the indents (nanodot average size ~95 nm), the relative closeness of the pits has led to a detachment of the metal layers between the indents, in the form of winding. On the contrary, the 2 µm-pitch array simultaneously exhibits the best indent filling and also good adhesion properties of the noble metal layer after the indentation process. As demonstrated in a previous work [1, 2], we argue that this optimum ordering occurs because the pattern pitch is comparable to the $SiO_xH_yC_z$ diffusion length (~1 µm).

1.2 Surface and volume vibrators analysis

In this part, a thorough Fourier Transformed Infra-Red spectroscopy in Specular Reflexion mode (SR-FTIR) study is performed on the $SiO_xH_yC_z$ nano-hillocks deposited on the 2 µm-pitch Pt/Si(100) pattern with the aim to directly correlate the Si-O-Si vibrators conformation with the morphological and chemical nano-islands properties (compactness, dimensions, native surface functionalization). SR-FTIR spectrum (Fig. 4) exhibits the characteristic features of amorphous silicon oxide films, namely $\delta_{Si\text{-}O\text{-}Si}$, $\gamma_{Si\text{-}O\text{-}Si}$, and $\nu_{as\ Si\text{-}O\text{-}Si}$ at 460, 805 and 1075 cm^{-1} respectively. The deconvolution of the ASM band (Asymmetric Stretching Mode, ~1000-1300 cm^{-1}) into Gaussian profiles gives rise to several couples of TO-LO (Transverse and Longitudinal Optical modes) vibrational modes. The first one, TO_1, appears at frequencies of 1072 cm^{-1} and corresponds to the asymmetrical vibrations of pure crystalline SiO_2, whose bond angle is 144°. According to [6], the frequency of TO_1 mode shifts towards higher wavenumber with rising stoichiometry x (SiO_x, x<2) from ~ 980 cm^{-1} for x=1 to ~1080 cm^{-1} for x=2. In the present case (1072 cm^{-1}), x can be roughly estimated to 1.8, indicating very low external contamination within the islands structure. In addition to the above-mentioned ASM component, three more modes are distinguished with maxima at around 1050, 1150 and 1200 cm^{-1} (corresponding to TO_3, TO_2, and LO_3 respectively). Contrary to the TO_1-LO_1 modes which reflect a quartz-like structure, the TO_3-LO_3 couple reveals planar threefold rings or packed fourfold rings configurations associated with average bond angles close to θ=120° (coesite-like structure). Then, a β-cristobalite-like structure revealed by a TO_2 mode at ~1150 cm^{-1} is associated with the higher bond angle θ=180°. This last mode, sometimes called surface mode, is characteristic of the specific surface within the film because of the numerous obtuse bond angles contained on the extreme surface. In the present case, its high convolution contribution (>20%) indicates a high degree of porosity or low compacity of the nano-islands, which is in consistent with SEM morphology (Fig. 3e.)

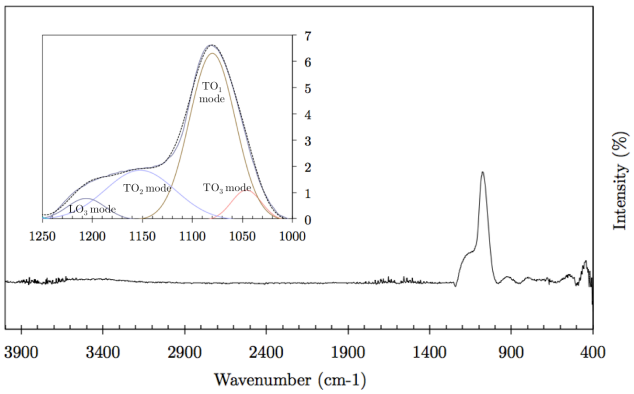

Figure 4: SR-FTIR spectrum of the $SiO_xH_yC_z$ films and magnification of deconvolution of the Si-O-Si ASM band profile into 4 modes of the SiOSi group.

1.3 Functionalization of the nano-islands

In addition to its remarkable ability to be functionalized by organic functions, in particular by azide and alkyne click reaction functions, silica is an interesting material for sensing applications thanks to its high –OH surface concentration (~ one each 5 $Å^2$), which gives it a great advantage in terms of sensibility. Thus the potential density of immobilized target biomolecules is relevant for the detection stage while the device can be miniaturized under the micrometric scale. On top of that, its chemical inertia and its mechanical strength in biological environment subjoin arguments for its integration on robust nano-biosensors.

In this part we report on the selective alkyno-functionalization of the nano-islands surface, followed by

the addition of coumarin fluorophore through click-chemistry process for a sensing purpose. Fine analysis of the nano-islands surface are performed by SR-FTIR mode in order to validate the success of the as-realized heterogeneous reactions.

According to published procedures, propargyl bromide (1) (Fig. 5) reacts under standard conditions with free/geminated –OH surface groups localized on the silica nano-island surface. After this first step, the as-obtained surface reacts the azido coumarin through click-reaction procedure reported elsewhere [7]. We expect that the specific fluorescence abilities of coumarin allow to visualize the nanoisland functionalization in the next steps of the nanosensor building.

Figure 5: chemical compounds used in this study

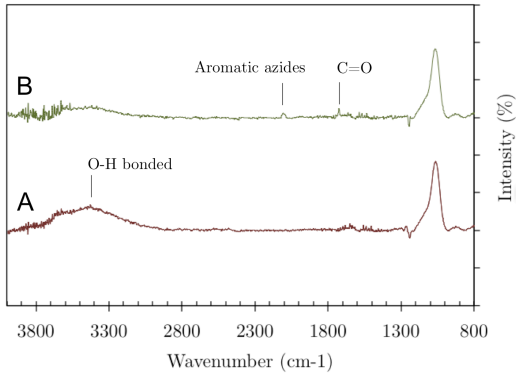

Figure 6: FT-IR analyses of the (A) un-functionalized silica nanodots and (B) coumarin-functionalized silica nanodots

Comparing the spectra of un-functionalized (A) and functionalized (B) silica nano-islands (Fig. 6) , the success of the click reaction was evidenced by the concommitant reduction of the OH band intensity (3000-3650 cm^{-1} - indicating that a major part of free/geminated OH have successfully reacted) and by the appearance of a band at 1731 cm^{-1} (C=O) corresponding to the coumarin signature. However, the band at 2100 cm^{-1} characteristic of azide aromatic vibrations could reveal that a minor part of the reactive coumarin solution remains captured within the island structure/porosity without being clicked.

4 CONCLUSION

Herein, we report on the spatial organization of $SiO_xH_yC_z$ nano-islands deposited on prepatterned Pt/Si(100) substrates with a microwave excited plasma torch operating at atmospheric pressure (Fig. 7). After comparison of the island ordering for several dimensionally ordered square arrays of indents, the 2 µ m-pitch array is selected and thoroughly examined by Specular Reflexion Fourier Transformed Infra-Red spectroscopy. Results demonstrates high level of internal porosity and –OH surface concentration. That way, this sample appears successively alkyno and azido-coumarin functionalized for sensing purpose through click-chemistry processes.

Further work should concentrate on both estimating the proportion of surface chemical groups through X-ray photoemission spectroscopy analysis and visualizing the functionalization through coumarin fluorescent properties in the far blue.

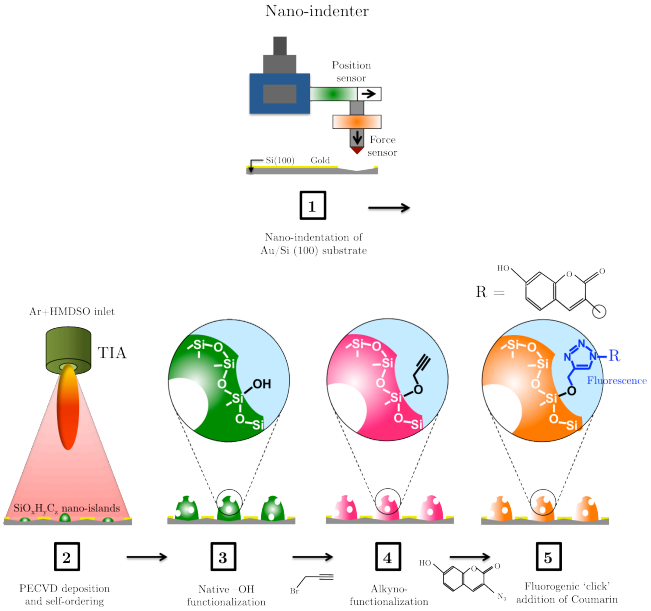

Figure 7: summary scheme of the study - from nano-indentation to selective azido-coumarin functionalization of silica-based nano-islands grown by PECVD at atmospheric pressure

REFERENCES

[1] X. Landreau, C. Dublanche-Tixier, C. Jaoul, C. Le Niniven, N. Lory, P. Tristant, Surf. Coat. Technol. 205, 335 (2011)

[2] X. Landreau, B. Lanfant, T. Merle, E. Laborde, C. Dublanche-Tixier, P. Tristant, Europ. Phys. J D 65 (3), 428 (2011)

[3] X. Landreau, P. Chagnon, C. Jaoul, C. Dublanche-Tixier, P. Tristant, Computational Materials Science 60, 32 (2012)

[4] X. Landreau, B. Lanfant, T. Merle, C. Dublanche-Tixier, P. Tristant, Europ. Phys. J D, accepted manuscript, (2012)

[5] H. Hu, H.J. Gao, F. Liu, Phys. Rev. Lett. 101, 216102 (2008)

[6] P.G. Pai, S.S. Chao, Y. Takagi, G. Lucovsky, J. Vac. Sci.Technol. 4, 690 (1986)

[7] P. Kele, X. Li, M. Link, K. Nagy, A. Herner, K. Lorincz, S. Beni, O.S. Wolfbeis, Org. Biomol. Chem. 7, 3490 (2009)